有机化学 DOI: 10.6023/cjoc202107024 研究论文
Chinese Journal of Organic Chemistry ARTICLE

Ag-Cu 负载的胺基石墨烯催化 β-羟基-1,2,3-三唑绿色合成研究

黄 强*,[a,b] 邓婷婷[a] 朱佳运[a] 李 军[a] 黎飞飞[a]
([a]遵义医科大学药学院 贵州遵义 563000)
([b]遵义医科大学基础药理教育部重点实验室 贵州遵义 563000)

摘要 开发了一种 Ag-Cu 双金属负载的胺基石墨烯催化剂用于 1,2,3-三唑类化合物的合成. 利用各种技术对催化剂进行了表征, 催化剂活性测试表明, 该催化剂在温和反应条件下具有高催化活性、好的循环稳定性和易分离的特点. 水作为绿色溶剂, 反应收率高. 该方法为 β-羟基-1,2,3-三唑类化合物的水相绿色合成提供了一种可替代的多相催化策略, 具有重要的科学价值.

关键词 石墨烯; 催化剂; 1,2,3-三唑; 点击化学; 多相催化

Study on the Green Synthesis of β-Hydroxy-1,2,3-triazoles Catalyzed by An Amino-Functionalized Graphene-Supported Ag-Cu Composites

Huang, Qiang*,[a,b] Deng, Tingting[a] Zhu, Jiayun[a] Li, Jun[a] Li, Feifei[a]
([a] *School of Pharmacy, Zunyi Medical University, Zunyi, Guizhou 563000*)
([b] *Key Laboratory of Basic Pharmacology of Ministry of Education, Zunyi Medical University, Zunyi, Guizhou 563000*)

Abstract An amino-functionalized graphene-immobilized Ag-Cu composite (Ag-Cu/GO-NH_2) was synthesized. The properties of the prepared catalyst were analyzed using various techniques, that showed high catalytic activity, good recyclability, and easy separability in the green synthesis of β-hydroxy-1,2,3-triazole derivatives under mild reaction conditions resulting in good to excellent yields. It provided an alternative heterogeneous catalytic strategy for the green synthesis of β-hydroxy-1,2,3-triazoles in water, which had an important scientific significance.

Keywords graphene; catalyst; 1,2,3-triazoles; click chemistry; heterogeneous catalysis

1 Introduction

1,2,3-Triazoles, an important class of five-membered nitrogen-containing heterocycles, have wide applications in various fields such as medicinal chemistry,[1] synthetic chemistry[2] and material science[3]. 1,2,3-Triazole skeletons as pharmacophores exhibited good biological properties, such as anticancer,[4] carbonic anhydrase inhibitors,[1c] and antibacterial activity,[5] which could be widely employed in the pharmaceutical development. Additionally, 1,2,3-triazoles could also be used as organic ligands in synthetic chemistry.[6] For example, Wang *et al.*[6a] reported indazolyl-pyridinyl-triazole iridium complex catalyzed the challenging selective reaction of benzylamines with arylamines in water. Given the importance of 1,2,3-triazoles, much effort has been devoted to develop high-efficient synthetic methods for the construction of 1,2,3-triazole derivatives.[7] For decades, the azide-alkyne Huisgen 1,3-dipolar cycloaddition was commonly considered as the main strategy led to the 1,2,3-triazole scaffold by click-chemistry reaction.[8] The homogeneous metal-catalyzed azide-alkyne cycloaddition has achieved considerable progresses in recent years.[9] The metal-based catalysts for the synthesis of 1,2,3-triazoles mainly included copper, silver or nickel complex.[10] For instance, Cu(II)-azide complex is an active catalyst for a three-component azide-epoxide-alkyne cycloaddition reaction in water.[10a] However, it was difficult to overcome some inherent shortcomings associ-

* Corresponding author. E-mail: huangqiang65@sina.com
Received July 10, 2021; revised September 27, 2021; published online October 14, 2021.
Project supported by the Academic Cultivation and Innovation Exploration Special Project of Zunyi Medical University in 2018 (Nos. [2018]5772-013, CK-1149-011), and the Young Talents Growth Project of the Higher Education Institutions of Guizhou Province (No. KY[2021]221).
遵义医科大学 2018 年学术新苗培养及创新探索专项(Nos. [2018]5772-013, CK-1149-011)、贵州省普通高等学校青年科技人才成长(No. KY[2021]221)资助项目.

ated with homogeneous catalytic systems, including the formation of metal-catalyzed homocoupling byproducts and the contamination of the target products by metal salts, which resulted in the need to recover and remove the catalyst. Hence, there are ongoing efforts to achieve the click synthesis of 1,2,3-triazoles by heterogeneous catalysis using hybrid materials such as metallic nanoparticles, mesoporous silica, graphene oxides (GO) or activated carbon and so on.[11]

Recently, functionalized graphene hybrids have attracted extensive attention for organic synthesis in the heterogeneous catalysis due to their good thermal stability, excellent catalytic performance, and dispersibility, including C—X coupling reactions[12] and click-chemistry reaction[13]. Especially, metal-graphene nanocomposites as catalysts were also well compatible for the formation of *N*-substituted 1,2,3-triazoles.[14] For example, Mirza-Aghayan's group reported that a Cu_2O/reduced graphene oxide/TiO_2 nanomaterial was utilized in "click" reaction for the synthesis of 1,4-disubstituted 1,2,3-triazoles via one pot multicomponent reaction of benzyl halide or epoxide derivatives with alkynes in presence of NaN_3 and triethylamine under visible light irradiation.[13c] This system characterized mild conditions, excellent yields of the triazole compounds, low catalyst loading and recoverability. Moreover, Schiff base functionalized GO Cu(II) complex was found to be highly efficient in the click reaction for the synthesis of 1,4-disubstituted 1,2,3-triazoles at room temperature, and the catalyst could be easily recycled up to successive four times without any noteworthy loss in the catalytic action.[14e] Despite these achievements that 1,2,3-triazoles were prepared by heterogeneous catalysis, the development of low-cost and high-efficient graphene-based catalysts to the synthesis of 1,2,3-triazoles is still extremely essential.

In our previous works, the amino-graphene copper hybrids could be employed for the C—N coupling reaction.[15] The heterogeneous catalysts showed low-cost, high-efficacy, recoverability, and recyclability that met the need of green chemistry. Therefore, we considered that these might be compatible for catalyzed synthesis of 1,2,3-triazoles by "click" reaction. To the best of our knowledge, Cu or Ag species could achieve excellent catalytic efficacy to efficiently sew terminal alkyne to azide to give triazole ring.[16] Some investigations suggested that bimetallic catalysts might be superior to the monometallic catalysts in the heterogeneous catalysis because of synergistic effect between the active components and the support.[17] For example, Paul's group reported a modified graphene supported Ag-Cu NPs with enhanced bimetallic synergistic effect in oxidation and Chan-Lam coupling reactions.[17a] Herein, it can be inferred that Ag-Cu bimetallic amino-graphene as a catalyst might be desirable for the synthesis of 1,2,3-triazoles. However, whether bimetallic Ag-Cu NPs supported on modified graphene can enhance catalytic activities or not, further studies should be conducted.

Keeping in view the above facts in mind, the amino-functionalized graphene-immobilized Ag-Cu composite (Ag-Cu/GO-NH_2) was prepared and systematically evaluated for one-pot three-component synthesis of 1,2,3-triazoles in water, so as to get insight into the role of bimetal nanoparticles and to explore the performance of catalyst.

2 Results and discussion

2.1 Characterization of Ag-Cu/GO-NH_2 nanohybrid

Firstly, In FT-IR spectra of GO-NH_2 (Figure 1a), the absorption band at 1728 and 1629 cm^{-1} can be assigned to the C=C and C=O stretching vibrations. The strong peaks at 3440 and 1398 cm^{-1} partially ascribe to absorbed water. After grafting amino acids on the GO material, the peaks at 1050, 1629, and 1728 cm^{-1} are attributed to characteristic amide bonds. The presence of a multiplet at 2922 cm^{-1} was associated with the stretching vibrations of CH_2. For the Ag-Cu/GO-NH_2 hybrid, when the Ag-Cu nanoparticles were immobilized on GO-NH_2 layers, the absorption band strength was weakened obviously, indicating the possible interaction between Ag-Cu nanoparticles and the grafted amino-functional groups on GO.

X-ray diffraction (XRD) of the GO-NH_2 and Ag-Cu/GO-NH_2 further confirmed the crystalline structures of the catalysts, as shown in Figure 1b. The presence of the Ag and Cu particles on the hybrid graphene material was evidenced by XRD, which shows the main peaks of Ag particles at 2θ of 38.1°, 43.4°, and 64.5° correspond to the expected diffraction angles by the (111), (200), and (220) planes of crystalline Ag, respectively. The peak at 44.4° and 77.6° correspond to (111) and (311) planes of crystalline Cu. The peak at 23.7° is attributed to graphene stacking.

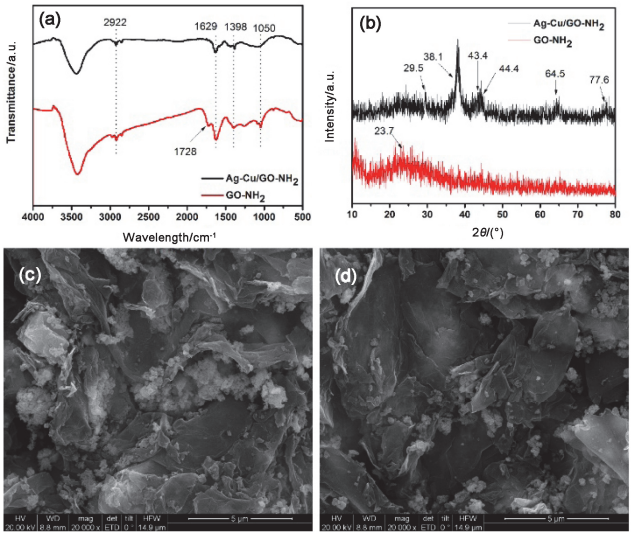

Figure 1 Caracterlization of catalysts by XRD, IR and SEM
(a) IR; (b) XRD; (c) and (d) SEM

The morphology of Ag-Cu/GO-NH_2 was studied by scanning electron microscopy (SEM). From SEM images (Figures 1c and 1d), it is observed that the Ag-Cu NPs an-

chored on GO-NH_2 are mainly dispersed at the periphery of graphene layers. A few Ag-Cu NPs aggregations are also observed in SEM images. The existence of Ag-Cu NPs at the periphery of amino-graphene sheets indicates that the binding of Ag-Cu NPs to GO-NH_2 is affected after functional modification.

2.2 Activity of Ag-Cu/GO-NH_2 catalyst

According to the Ag or Cu salts promoted the click reaction basing on the previous researches,[8] the performance of the Ag-Cu/GO-NH_2 catalyst was evaluated. A three-component reaction of alkenyl oxide, sodium azide (NaN_3), and terminal alkynes was conducted for the synthesis of 1,4-disubstituted 1,2,3-triazoles (**3a**). The initially reaction of alkenyl oxide, NaN_3, and phenylacetylene was selected as a model for optimizing the conditions. As seen from Table 1, delightfully, the reaction could proceed with 73% isolated yield using 5 mg of Ag-Cu/GO-NH_2 catalyst at 80 ℃ in H_2O. However, organic solvents were not conducive to improve the yield of **3a** (Enteries 1～5). The main reason might be the poor solubility and low ionization of NaN_3. Next, the screening of reaction temperature indicated that significantly improved reaction efficiency could be obtained at 50 ℃ (Entries 6～10). Finally, Ag-Cu/GO-NH_2 catalyst loading was further examined. The reaction efficiency was slightly improved along with the reduction of catalyst loading, and 2 mg of Ag-Cu/GO-NH_2 was found to be the best choice (Entries 11～14). However, when the loading was further reduced to 1 mg or none of catalyst, it resulted to significant loss-efficiency (Entries 15～16).

Table 1 Optimization of the reaction conditions[a]

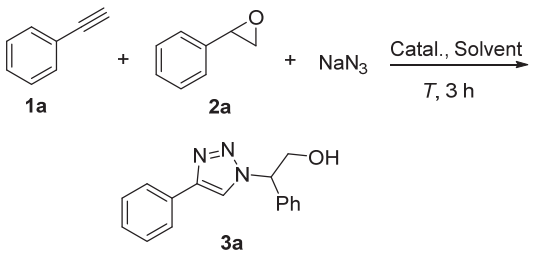

Entry	Catalyst (loading/mg)	T/℃	Solvent	Yield[b]/%
1	Ag-Cu/GO-NH_2 (5)	80	EtOH	16
2	Ag-Cu/GO-NH_2 (5)	80	MeOH	12
3	Ag-Cu/GO-NH_2 (5)	80	H_2O	73
4	Ag-Cu/GO-NH_2 (5)	80	CH_3CN	ND
5	Ag-Cu/GO-NH_2 (5)	80	DMF	ND
6	Ag-Cu/GO-NH_2 (5)	70	H_2O	81
7	Ag-Cu/GO-NH_2 (5)	60	H_2O	85
8	Ag-Cu/GO-NH_2 (5)	50	H_2O	87
9	Ag-Cu/GO-NH_2 (5)	40	H_2O	68
10	Ag-Cu/GO-NH_2 (5)	25	H_2O	26
11	Ag-Cu/GO-NH_2 (6)	50	H_2O	88
12	Ag-Cu/GO-NH_2 (4)	50	H_2O	87
13	Ag-Cu/GO-NH_2 (3)	50	H_2O	89
14	Ag-Cu/GO-NH_2 (2)	50	H_2O	91
15	Ag-Cu/GO-NH_2 (1)	50	H_2O	72
16	—	50	H_2O	ND

[a] Reaction conditions: **1a** (1 mmol), **2a** (1 mmol), NaN_3 (1.2 mmol), catalyst (2～6 mg), reaction time (3 h), solvent (4 mL), atmosphere. [b] Isolated yields.

With the optimized conditions in hand, the scope of substrates was explored. As shown in Scheme 1, various substituted alkynes were examined in this synthesis of 1,4-disubstituted 1,2,3-triazoles (**3a** ～ **3o**). Most of *para*-substituted phenylacetylene smoothly reacted with styrene oxide and sodium azide, giving the corresponding products in excellent yields (**3b**～**3i**). The electronic effect and steric hindrance of substituents have a slight effect on the reaction efficiency. While *p*- or *o*-chlorophenylacetylene was conducted (**3c** and **3k**), a medium yield was obtained, which might be due to the self-coupling reaction occurred. Notably, heterocycle and alkyl terminal alkynes were also compatible for the reaction, and the corresponding products (**3l**～**3o**) were afforded in excellent yields. Next, different epoxides were examined. Most epoxides were suitable for this system, and the desired products were also afforded in good yields (**3p**～**3u**). Substituent groups have not obvious effect on the reactivity of epoxides. The obtained 1,4-disubstituted 1,2,3-triazoles might have potential bioactivities and be employed in medicinal chemistry.

To evaluate the recyclability of this catalyst, the repeated experiment was conducted. As shown in Figure 2, the as-prepared Ag-Cu/GO-NH_2 catalyst can be used five times with slight decrease of catalytic activity, which indicated good stability. Here, inductively coupled plasma mass spectrometer (ICP-MS) analyzed the concentration of metal ions in the reaction solution from leaching of Ag-Cu/GO-NH_2. It was found that the solution contained 0.4524 μg/mL Ag and 0.4454 μg/mL Cu ions after first recovery, which can calculate that the Ag and Cu species leaching rates of catalyst are about 2% and 5% by reused five times, respectively, which might be the main reason leading to slight decrease of catalytic activity.

Finally, in order to get insight into the role of bimetal NPs and explore the performance of catalyst, the monometallic Ag/GO-NH_2 and Cu/GO-NH_2 hybrids were fabricated under standard conditions, and then different catalytic systems were compared for the synthesis of *β*-hydroxy-1,2,3-triazoles. As seen from Table 2, the corresponding Cu or Ag salts as homogeneous catalysts just showed extremely catalytic performance. In contrast, heterogeneous catalysts could obviously enhance the reaction efficiency. However, compared with Ag-Cu/GO-NH_2, lower catalytic activities were observed when monometallic Cu/GO-NH_2 or Ag/GO-NH_2 catalysts was used. Transmission electron microscopy (TEM) analyzed the nanostructures of different catalysts in Figure 3. It found that the size of Ag or Cu NPs supported on the GO-NH_2 is about 20 nm. The morphology of Cu NPs was amorphous in the Cu/GO-NH_2 hybrid. When the Ag and Cu species were both immobilized on the GO-NH_2, the smaller size of NPs (about 10 nm) could be obtained. Interestingly, the nanostructures

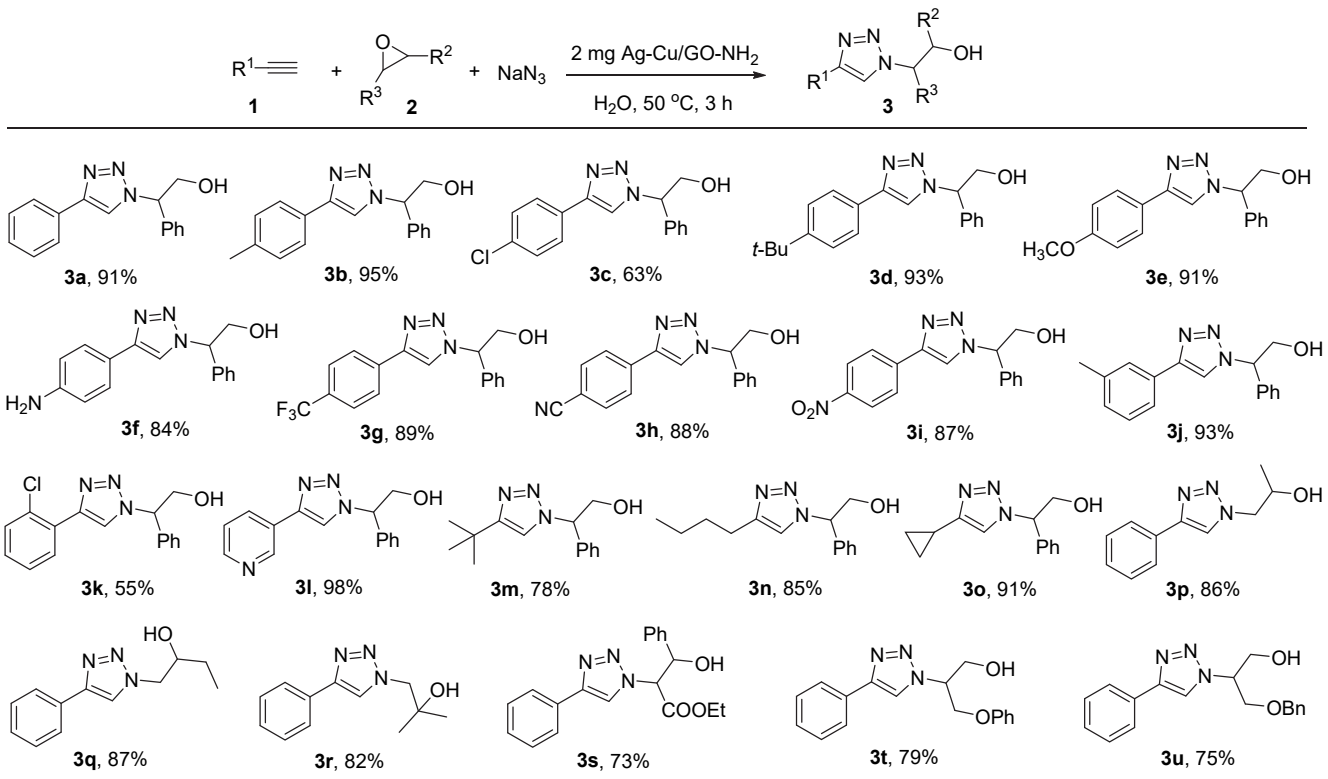

Scheme 1 Scope of substituted alkynes and epoxides

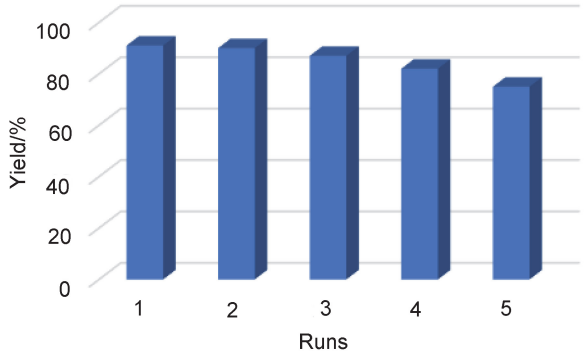

Figure 2 Reusabilities of Ag-Cu/GO-NH_2 catalyst

and the morphology of Ag-Cu NPs without significant changes could be still supported on the GO-NH_2 after reuse five times, which indicated good stability. According to the above all, it concluded that the existence of synergistic effect between Ag and Cu NPs would increase the surface area available for reaction system and improve the surface exposure of the catalytic active sites. Hence, bimetallic Ag-Cu/GO-NH_2 catalyst showed higher reaction efficiency. Additionally, compared to other heterogeneous catalysts, such as Cu-coordinated DADO-functionalized graphene oxide (GO-DADO-Cu),[11f] the Ag-Cu/GO-NH_2 catalyst has a better catalytic performance.

2.3 Mechanism of catalytic reaction

Generally, the complete mechanism of the heterogeneous catalysis is not fully clear. However, on the basis of the above control experiments in Table 2 and the reported

Table 2 Comparison of various catalysts for the synthesis of *β*-hydroxy-1,2,3-triazoles

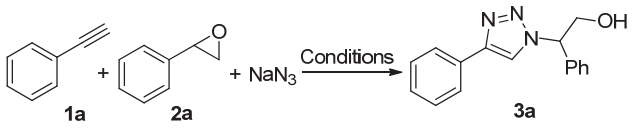

Entry	Catalyst	Conditions	Yield[a]/%
1	Ag-Cu/GO-NH_2	2 mg, 50 ℃, H_2O, 3 h	91
2	Ag_2CO_3	5 mg, 50 ℃, H_2O, 3 h	18
3	$Cu(CH_3COO)_2•H_2O$	5 mg, 50 ℃, H_2O, 3 h	15
4	$AgNO_3$	5 mg, 50 ℃, H_2O, 3 h	17
5	Ag/GO-NH_2	2 mg, 50 ℃, H_2O, 3 h	21
6	Cu/GO-NH_2	2 mg, 50 ℃, H_2O, 3 h	78

[a] Isolated yield by silica gel chromatography. Conditions: **1a** (1 mmol), **2a** (1 mmol), NaN_3 (1.2 mmol), catalyst (2 mg/5 mg), reaction time 3 h, H_2O (4 mL), atmosphere.

mechanisms for the synthesis of triazoles catalyzed by copper complexes,[18] the plausible mechanism for the synthesis of 1,2,3-triazoles might follow the pathway as shown in Scheme 2. In the first step, the azide coordinated to the Ag-Cu NPs was involved in the nucleophilic attack to epoxystyrene, which formed complex **1**. Next, Ag-Cu NPs activated the terminal alkyne by generating transient alkynyl bimetallic intermediate complex **2**, and then facilitated the cyclization reaction between alkyl-azide and arylacetylene which was coordinated to the Ag-Cu center. After cycloaddition, protonolysis of the complex **3** by aqueous media afforded the corresponding 1,2,3-triazoles.

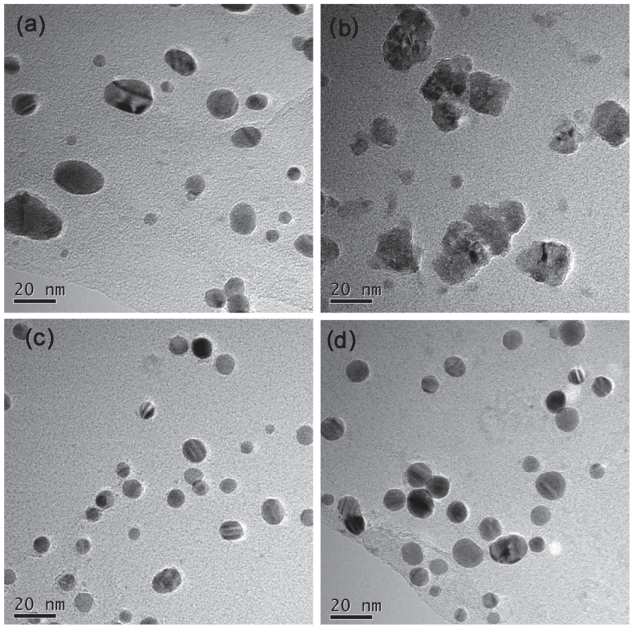

Figure 3 Pattern of TEM analysis for different catalysts
(a) Ag/GO-NH_2; (b) Cu/GO-NH_2; (c) Ag-Cu/GO-NH_2; (d) reused Ag-Cu/GO-NH_2

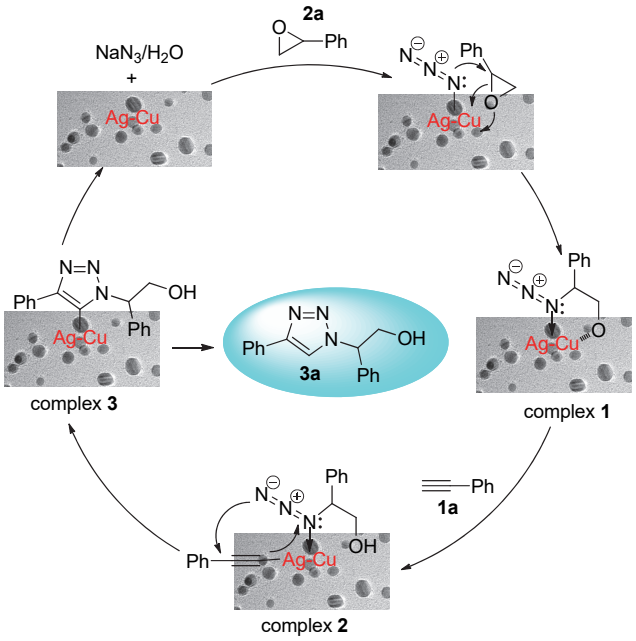

Scheme 2 Proposed mechanism for the synthesis of 1,2,3-triazoles in the absence of NaN_3 and H_2O

According to these results, the present catalytic system appears to be more efficient in the green synthesis of *β*-hydroxy-1,2,3-triazoles for several reasons: (i) the existence of bimetal synergistic effect between Ag and Cu NPs would improve the surface exposure of the catalytic active sites, (ii) amino-functionalized graphene might facilitate the better immobilization of the Ag-Cu NPs active centers, and (iii) the bimetal nanoparticles might enhance the stability of catalyst. Hence, compared with homogeneous catalysts, the Ag-Cu/GO-NH_2 with simple synthesis, easy separation and recyclability have potential values in practical application.

3 Conclusions

In summary, a new heterogeneous catalytic system was developed for the green click synthesis of *β*-hydroxy-1,2,3-triazoles using Ag-Cu/GO-NH_2 catalyst. Various 1,2,3-triazole derivatives were produced in good yields. This Ag-Cu/GO-NH_2 nanohybrid showed high catalytic activity and good recyclability. Compared with homogeneous reaction, the heterogeneous catalytic system was very benefit to isolate product and recycle of catalyst, which might be of great importance for practical application.

4 Experimental section

4.1 Materials and characterization

GO was purchased from Nanjing XFNANO Materials Tech Co.; $Cu(CH_3COO)_2•H_2O$ and $AgNO_3$ were obtained from Sinopharm Chemical Reagent Co. Ltd. (Shanghai, China). $NaBH_4$ and solvents were purchased from Kelong Chemical Reagent Co. Ltd. (Chengdu China). The deionized (DI) water used throughout all experiments was purified to 18.2 MXm with the Millipore system. All reagents were of analytical grade and were used as received. The catalyst was characterized by Scanning Electron Microscopy (SEM, AJEOL JSM-6510LV, JAPAN) and X-Ray Diffraction (XRD, D/MAX Ultima IV, JAPAN). Fourier transform infrared (FT-IR) spectroscopy was performed on a Perkin-Elmar model 2000 FT-IR spectrophotometer using the Spectrum v. 2.00 software package. Analytical thin layer chromatography (TLC) was performed on percolated silica gel 60 F254 plates. ^1H NMR and ^{13}C NMR spectra were recorded in $CDCl_3$ with tetra-methylsilane (TMS) as the internal standard. Column chromatography was conducted on columns of silica gel (200～300 mesh).

4.2 Synthesis of catalyst

GO (100 mg) was added in 500 mL of *N*,*N*-dimethylformamide (DMF), and then sonicated for 60 min to give the homogeneous suspension. 4-Amino-2,2,6,6-tetramethylpiperidine (10 mmol, 1.58 g), *O*-(7-azabenzotriazol-1-yl)-*N*,*N*,*N*′,*N*′-tetra-methyluronium hexafluorophosphate (HATU, 10 mmol, 3.8 g) and Et_3N (20 mmol, 2.02 g) were added into the mixture by stirring. The mixture kept warm at 30 ℃ for 48 h until completion of reaction. Then the solid was isolated by vacuum filtration and filter cake was washed with distilled water repeatedly. Finally, the obtained solid was dispersed into 500 mL of H_2O again to obtain the GO-NH_2 solution.

$Cu(CH_3COO)_2•H_2O$ solution (10 mmol/L, 20 mL) and $AgNO_3$ solution (10 mmol/L, 30 mL) were dropped into GO-NH_2 suspension by the constant flow pump, respectively, and then sonicated for 30 min. Next, the 50 mL of 2.0 mg•mL^{-1} $NaBH_4$ solution was added dropwise into the

above solution. After completion of reaction, the obtained solid was filtrated and washed with water and ethanol, respectively. Finally, the prepared catalyst (Ag-Cu/GO-NH_2) was dried at 50 ℃ for 24 h under N_2. The loadings of Ag and Cu species were calculated about 22 and 9 wt% in theory.

For the Ag/GO-NH_2 and Cu/GO-NH_2 catalysts, the synthetic procedures were the same with Ag-Cu/GO-NH_2.

4.3 Synthesis of β-hydroxy-1,2,3-triazoles

A three-component reaction of alkenyl oxide (**2**, 1.0 mmol), sodium azide (NaN_3, 1.2 mmol), and terminal alkynes (**1**, 1.0 mmol) was conducted stirring at setting temperature for 3 h in an atmosphere. After the completion of reaction, the mixture was diluted with H_2O (20 mL), and extracted with ethyl acetate (10 mL×3). The combined organic layers were washed with saturated brine twice, and dried over anhydrous Na_2SO_4. After filtration, the solvent was evaporated in vacuo. The crude product was purified by silica gel chromatography [*V*(petroleum ether)∶*V*(ethyl acetate)=10∶1～5∶1] to give the desired compounds.

4.4 Recoverability of catalyst

Phenylacetylene (**1a**, 5 mmol), styrene oxide (**2a**, 5 mmol), sodium azide (NaN_3, 6 mmol), catalyst (10 mg), and H_2O (20 mL) were added into a 50 mL round-bottomed flask and stirring at setting temperature for 3 h in an air atmosphere. After the completion of reaction, the mixture was centrifuged to separate the solid and H_2O phase. The solid was washed with ethyl acetate (10 mL×3) by filtration. The filtrate was dried over anhydrous Na_2SO_4. After filtration, the solvent was evaporated in vacuo. The crude product was purified by silica gel chromatography [*V*(petroleum ether)∶*V*(ethyl acetate)=10∶1] to give the desired compound **3a**. The recovered catalyst was collected from filter cake and dried for 12 h under vacuum oven, and then reused in the next reaction.

2-Phenyl-2-(4-phenyl-1*H*-1,2,3-triazol-1-yl)ethan-1-ol (**3a**): 242 mg, white solid, 91% yield. m.p. 130～132 ℃; ^{1}H NMR (400 MHz, $CDCl_3$) *δ*: 7.79～7.74 (m, 2H), 7.73 (s, 1H), 7.44～7.29 (m, 8H), 5.71 (dd, *J*=8.3, 3.7 Hz, 1H), 4.66 (ddd, *J*=13.2, 8.3, 5.2 Hz, 1H), 4.25 (ddd, *J*=12.2, 8.3, 3.7 Hz, 1H), 3.92～3.72 (m, 1H); ^{13}C NMR (101 MHz, $CDCl_3$) *δ*: 147.63, 136.07, 130.17, 129.16, 128.99, 128.84, 128.49, 128.30, 127.18, 126.11, 125.68, 120.63, 67.37, 65.06; HRMS (ESI) calcd for $C_{16}H_{16}N_3O$ $[M+H]^+$ 265.1215, found 265.1219.

2-Phenyl-2-(4-(*p*-tolyl)-1*H*-1,2,3-triazol-1-yl)ethan-1-ol (**3b**): 265 mg, white solid, 95% yield. m.p. 127～128 ℃; ^{1}H NMR (400 MHz, $CDCl_3$) *δ*: 7.69 (s, 1H), 7.67 (s, 2H), 7.44～7.38 (m, 3H), 7.31～7.26 (m, 2H), 7.23 (d, *J*=8.0 Hz, 2H), 5.69 (dd, *J*=8.3, 3.7 Hz, 1H), 4.70～4.61 (m, 1H), 4.24 (ddd, *J*=12.5, 8.8, 3.8 Hz, 1H), 3.50 (dd, *J*=8.8, 5.4 Hz, 1H), 2.39 (s, 3H); ^{13}C NMR (101 MHz, $CDCl_3$) *δ*: 147.84, 138.19, 136.11, 129.52, 129.18, 129.02, 128.84, 127.40, 127.15, 125.92, 125.60, 120.23, 67.28, 65.25, 21.31; HRMS (ESI) calcd for $C_{17}H_{18}N_3O$ $[M+H]^+$ 279.1372, found 279.1369.

2-(4-(4-Chlorophenyl)-1*H*-1,2,3-triazol-1-yl)-2-phenylethan-1-ol (**3c**): 188 mg, white solid, 63% yield. m.p. 128～129 ℃; ^{1}H NMR (400 MHz, $CDCl_3$) *δ*: 7.75 (d, *J*=7.8 Hz, 2H), 7.72 (s, 1H), 7.47～7.37 (m, 5H), 7.31～7.27 (m, 2H), 5.70 (dd, *J*=8.2, 3.7 Hz, 1H), 4.71～4.61 (m, 1H), 4.30～4.21 (m, 1H), 3.22～3.09 (m, 1H); ^{13}C NMR (101 MHz, $CDCl_3$) *δ*: 146.81, 135.88, 134.10, 129.28, 129.17, 129.07, 127.13, 126.95, 120.61, 67.34, 65.23; HRMS (ESI) calcd for $C_{16}H_{15}ClN_3O$ $[M+H]^+$ 299.0825, found 299.0822.

2-(4-(4-(*tert*-Butyl)phenyl)-1*H*-1,2,3-triazol-1-yl)-2-phenylethan-1-ol (**3d**): 299 mg, white solid, 93% yield. m.p. 131～132 ℃; ^{1}H NMR (400 MHz, $CDCl_3$) *δ*: 7.75～7.70 (m, 2H), 7.69 (s, 1H), 7.49～7.36 (m, 5H), 7.31～7.24 (m, 2H), 5.70 (dd, *J*=8.2, 3.7 Hz, 1H), 4.75～4.62 (m, 1H), 4.25 (ddd, *J*=12.4, 8.7, 3.7 Hz, 1H), 3.65～3.40 (m, 1H), 1.36 (s, 9H); ^{13}C NMR (101 MHz, $CDCl_3$) *δ*: 151.45, 147.76, 136.15, 129.17, 129.00, 127.38, 127.12, 125.76, 125.43, 120.33, 67.28, 65.27, 34.68, 31.29; HRMS (ESI) calcd for $C_{20}H_{24}N_3O$ $[M+H]^+$ 321.1841, found 321.1845.

2-(4-(4-Methoxyphenyl)-1*H*-1,2,3-triazol-1-yl)-2-phenylethan-1-ol (**3e**): 269 mg, white solid, 91% yield. m.p. 137～138 ℃; ^{1}H NMR (400 MHz, $CDCl_3$) *δ*: 7.73～7.65 (m, 2H), 7.63 (s, 1H), 7.45～7.37 (m, 3H), 7.33～7.25 (m, 2H), 6.94 (d, *J*=8.8 Hz, 2H), 5.68 (dd, *J*=8.3, 3.7 Hz, 1H), 4.69～4.60 (m, 1H), 4.29～4.20 (m, 1H), 3.85 (s, 3H), 3.82～3.65 (m, 1H); ^{13}C NMR (101 MHz, $CDCl_3$) *δ*: 159.67, 147.55, 136.13, 129.15, 128.98, 127.16, 127.00, 122.92, 119.79, 114.23, 67.30, 65.18, 55.33; HRMS (ESI) calcd for $C_{17}H_{18}N_3O_2$ $[M+H]^+$ 295.1321, found 295.1325.

2-(4-(4-Aminophenyl)-1*H*-1,2,3-triazol-1-yl)-2-phenylethan-1-ol (**3f**): 235 mg, gray solid, 84% yield. m.p. 127～128 ℃; ^{1}H NMR (400 MHz, $CDCl_3$) *δ*: 7.64～7.48 (m, 3H), 7.44～7.36 (m, 3H), 7.29～7.23 (m, 2H), 6.73 (d, *J*=8.4 Hz, 2H), 5.66 (dd, *J*=8.2, 3.6 Hz, 1H), 4.70～4.60 (m, 1H), 4.30～4.17 (m, 1H), 3.79 (s, 2H), 3.50 (s, 1H); ^{13}C NMR (101 MHz, $CDCl_3$) *δ*: 148.11, 146.60, 136.21, 129.15, 128.96, 127.12, 126.94, 120.73, 119.28, 115.24, 67.18, 65.28; HRMS (ESI) calcd for $C_{16}H_{17}N_4O$ $[M+H]^+$ 280.1324, found 280.1320.

2-Phenyl-2-(4-(4-(trifluoromethyl)phenyl)-1*H*-1,2,3-triazol-1-yl)ethan-1-ol (**3g**): 296 mg, white solid, 89% yield. m.p. 110～111 ℃; ^{1}H NMR (400 MHz, $CDCl_3$) *δ*: 7.93～7.86 (m, 2H), 7.82 (s, 1H), 7.67 (d, *J*=7.9 Hz, 2H), 7.48～7.38 (m, 3H), 7.35～7.29 (m, 2H), 5.73 (dd, *J*=8.1, 3.7 Hz, 1H), 4.74～4.63 (m, 1H), 4.32～4.23 (m, 1H), 3.35 (d, *J*=52.7 Hz, 1H); ^{13}C NMR (101 MHz, $CDCl_3$) *δ*: 146.36, 135.76, 133.66, 129.29, 129.21, 127.17, 126.40～125.68 (m), 125.78, 121.35, 67.47, 65.13; HRMS (ESI) calcd for $C_{17}H_{15}F_3N_3O$ $[M+H]^+$ 333.1089, found 333.1085.

4-(1-(2-Hydroxy-1-phenylethyl)-1*H*-1,2,3-triazol-4-yl)-benzonitrile (**3h**): 255 mg, white solid, 88% yield. m.p. 121～122 ℃; ^{1}H NMR (400 MHz, $CDCl_3$) *δ*: 7.94～7.88 (m, 2H), 7.86 (s, 1H), 7.73～7.68 (m, 2H), 7.45～7.39 (m,

3H), 7.34～7.28 (m, 2H), 5.74 (dd, J=8.1, 3.8 Hz, 1H), 4.73～4.62 (m, 1H), 4.33～4.21 (m, 1H), 3.31～3.21 (m, 1H); ^{13}C NMR (101 MHz, $CDCl_3$) δ: 145.94, 135.64, 134.65, 132.74, 129.33, 129.28, 127.14, 126.07, 121.73, 118.70, 111.65, 67.47, 65.03; HRMS (ESI) calcd for $C_{17}H_{15}N_4O$ $[M+H]^+$ 290.1168, found 290.1165.

2-(4-(4-Nitrophenyl)-1*H*-1,2,3-triazol-1-yl)-2-phenylethan-1-ol (**3i**): 270 mg, gray solid, 87% yield. m.p. 130～131 ℃; ^{1}H NMR (400 MHz, $CDCl_3$) δ: 8.28 (d, J=8.8 Hz, 2H), 7.98 (d, J=8.8 Hz, 2H), 7.92 (s, 1H), 7.48～7.39 (m, 3H), 7.34～7.29 (m, 2H), 5.76 (dd, J=8.1, 3.8 Hz, 1H), 4.68 (ddd, J=13.1, 8.1, 5.4 Hz, 1H), 4.29 (ddd, J=12.2, 8.2, 3.8 Hz, 1H), 3.25～3.10 (m, 1H); ^{13}C NMR (101 MHz, $CDCl_3$) δ: 147.40, 145.60, 136.52, 135.59, 129.35, 129.31, 127.16, 126.17, 124.32, 122.06, 67.51, 65.01; HRMS (ESI) calcd for $C_{16}H_{15}N_4O_3$ $[M+H]^+$ 310.1066, found 310.1070.

2-Phenyl-2-(4-(*m*-tolyl)-1*H*-1,2,3-triazol-1-yl)ethan-1-ol (**3j**): 260 mg, white solid, 93% yield. m.p. 115～116 ℃; ^{1}H NMR (400 MHz, $CDCl_3$) δ: 7.70 (s, 1H), 7.65～7.54 (m, 2H), 7.46～7.36 (m, 3H), 7.35～7.24 (m, 3H), 7.16 (d, J=7.6 Hz, 1H), 5.70 (dd, J=8.2, 3.7 Hz, 1H), 4.66 (ddd, J=13.4, 8.2, 5.4 Hz, 1H), 4.25 (ddd, J=12.4, 8.7, 3.7 Hz, 1H), 3.69～3.48 (m, 1H), 2.40 (s, 3H); ^{13}C NMR (101 MHz, $CDCl_3$) δ: 147.84, 138.51, 136.09, 130.08, 129.18, 129.08, 129.02, 128.74, 127.15, 126.37, 122.79, 120.55, 67.30, 65.20, 21.43; HRMS (ESI) calcd for $C_{17}H_{18}N_3O$ $[M+H]^+$ 279.1372, found 279.1370.

2-(4-(2-Chlorophenyl)-1*H*-1,2,3-triazol-1-yl)-2-phenylethan-1-ol (**3k**): 164 mg, white solid, 55% yield. m.p. 107～108 ℃; ^{1}H NMR (400 MHz, $CDCl_3$) δ: 8.22 (dd, J=7.8, 1.5 Hz, 1H), 8.16 (s, 1H), 7.46～7.35 (m, 5H), 7.32～7.24 (m, 3H), 5.75 (dd, J=8.3, 3.9 Hz, 1H), 4.73～4.59 (m, 1H), 4.26 (d, J=12.1 Hz, 1H), 3.57 (s, 1H); ^{13}C NMR (101 MHz, $CDCl_3$) δ: 144.01, 136.04, 131.28, 130.22, 129.72, 129.16, 128.99, 128.94, 127.18, 127.09, 124.18, 67.36, 65.15; HRMS (ESI) calcd for $C_{16}H_{15}ClN_3O$ $[M+H]^+$ 299.0825, found 299.0827.

2-Phenyl-2-(4-(pyridin-3-yl)-1*H*-1,2,3-triazol-1-yl)-ethan-1-ol (**3l**): 261 mg, gray solid, 98% yield. m.p. 115～116 ℃; ^{1}H NMR (400 MHz, $CDCl_3$) δ: 8.96 (d, J=1.6 Hz, 1H), 8.57 (dd, J=4.8, 1.6 Hz, 1H), 8.23～8.16 (m, 1H), 7.85 (s, 1H), 7.46～7.40 (m, 3H), 7.40～7.35 (m, 1H), 7.34～7.30 (m, 2H), 5.75 (dd, J=8.2, 3.8 Hz, 1H), 4.72～4.63 (m, 1H), 4.32～4.22 (m, 1H), 3.37 (s, 1H); ^{13}C NMR (101 MHz, $CDCl_3$) δ: 149.30, 146.97, 144.75, 135.80, 133.04, 129.30, 129.21, 127.14, 126.51, 123.79, 120.91, 67.45, 65.11; HRMS (ESI) calcd for $C_{15}H_{15}N_4O$ $[M+H]^+$ 266.1168, found 266.1165.

2-(4-(*tert*-Butyl)-1*H*-1,2,3-triazol-1-yl)-2-phenylethan-1-ol (**3m**): 191 mg, viscose oil, 78% yield. ^{1}H NMR (400 MHz, $CDCl_3$) δ: 7.42～7.28 (m, 4H), 7.25～7.20 (m, 2H), 5.63 (dd, J=8.3, 3.2 Hz, 1H), 4.57 (dd, J=11.8, 8.6 Hz, 1H), 4.17 (dd, J=12.4, 3.7 Hz, 2H), 1.32 (s, 9H); ^{13}C NMR (101 MHz, $CDCl_3$) δ: 157.50, 136.48, 129.03, 128.76, 128.64, 128.37, 127.70, 127.12, 126.14, 125.96, 119.53, 67.00, 65.06, 30.31; HRMS (ESI) calcd for $C_{14}H_{20}N_3O$ $[M+H]^+$ 245.1528, found 245.1531.

2-(4-Butyl-1*H*-1,2,3-triazol-1-yl)-2-phenylethan-1-ol (**3n**): 208 mg, viscose oil, 85% yield. ^{1}H NMR (400 MHz, $CDCl_3$) δ: 7.35 (s, 1H), 7.34～7.29 (m, 3H), 7.24～7.20 (m, 2H), 5.66 (dd, J=8.3, 4.2 Hz, 1H), 4.56～4.45 (m, 1H), 4.21～4.12 (m, 1H), 2.68～2.59 (m, 2H), 1.57 (dd, J=15.4, 7.8 Hz, 2H), 1.33 (dd, J=14.9, 7.4 Hz, 2H), 0.89 (t, J=7.3 Hz, 3H); ^{13}C NMR (101 MHz, $CDCl_3$) δ: 148.05, 136.58, 128.92, 128.63, 127.09, 121.49, 66.91, 64.59, 31.36, 25.25, 22.32, 13.82; HRMS (ESI) calcd for $C_{14}H_{20}N_3O$ $[M+H]^+$ 245.1528, found 245.1530.

2-(4-Cyclopropyl-1*H*-1,2,3-triazol-1-yl)-2-phenylethan-1-ol (**3o**): 209 mg, viscose oil, 91% yield. ^{1}H NMR (400 MHz, $CDCl_3$) δ: 7.34 (s, 1H), 7.32～7.26 (m, 3H), 7.25～7.18 (m, 2H), 5.64 (dd, J=8.4, 4.3 Hz, 1H), 4.90 (s, 1H), 4.46 (dd, J=12.1, 8.5 Hz, 1H), 4.14 (dd, J=12.1, 4.2 Hz, 1H), 1.91～1.79 (m, 1H), 0.92～0.82 (m, 2H), 0.80～0.67 (m, 2H); ^{13}C NMR (101 MHz, $CDCl_3$) δ: 149.87, 136.47, 128.91, 128.63, 127.13, 120.59, 66.90, 64.41, 7.78, 6.63; HRMS (ESI) calcd for $C_{13}H_{16}N_3O$ $[M+H]^+$ 229.1215, found 229.2220.

1-(4-Phenyl-1*H*-1,2,3-triazol-1-yl)propan-2-ol (**3p**): 175 mg, white solid, 86% yield. m.p. 119～120 ℃; ^{1}H NMR (400 MHz, $CDCl_3$) δ: 7.86 (s, 1H), 7.80～7.70 (m, 2H), 7.45～7.37 (m, 2H), 7.38～7.30 (m, 1H), 4.50 (d, J=13.8 Hz, 1H), 4.45～4.32 (m, 1H), 4.31～4.20 (m, 1H), 3.50～3.10 (m, 1H), 1.35 (d, J=6.2 Hz, 3H); ^{13}C NMR (101 MHz, $CDCl_3$) δ: 130.31, 128.82, 128.14, 125.57, 66.68, 57.37, 20.51; HRMS (ESI) calcd for $C_{11}H_{14}N_3O$ $[M+H]^+$ 203.1059, found 203.1055.

1-(4-Phenyl-1*H*-1,2,3-triazol-1-yl)butan-2-ol (**3q**): 189 mg, white solid, 87% yield. m.p. 145～146 ℃; ^{1}H NMR (400 MHz, $CDCl_3$) δ: 7.88～7.81 (m, 1H), 7.81～7.68 (m, 2H), 7.45～7.30 (m, 3H), 4.58～4.46 (m, 1H), 4.34～4.19 (m, 1H), 4.17～4.03 (m, 1H), 3.54～3.00 (m, 1H), 1.70～1.54 (m, 2H), 1.09 (t, J=7.4 Hz, 3H); ^{13}C NMR (101 MHz, $CDCl_3$) δ: 147.35, 130.33, 128.81, 128.10, 125.56, 121.17, 71.77, 55.96, 27.49, 9.85; HRMS (ESI) calcd for $C_{11}H_{14}N_3O$ $[M+H]^+$ 217.1215, found 217.1212.

2-Methyl-1-(4-phenyl-1*H*-1,2,3-triazol-1-yl)propan-2-ol (**3r**): 178 mg, white solid, 82% yield. m.p. 89～91 ℃; ^{1}H NMR (400 MHz, $CDCl_3$) δ: 7.96 (s, 1H), 7.86 (d, J=7.3 Hz, 2H), 7.45 (t, J=7.5 Hz, 2H), 7.36 (t, J=7.3 Hz, 1H), 4.40 (s, 2H), 2.51 (d, J=29.6 Hz, 1H), 1.30 (s, 6H); ^{13}C NMR (101 MHz, $CDCl_3$) δ: 130.52, 128.86, 128.18, 125.71, 121.44, 70.46, 60.50, 27.16; HRMS (ESI) calcd for $C_{12}H_{16}N_3O$ $[M+H]^+$ 217.1215, found 217.1212.

Ethyl 3-hydroxy-3-phenyl-2-(4-phenyl-1*H*-1,2,3-triazol-1-yl) propanoate (**3s**): 246 mg, white solid, 73% yield. m.p. 128～129 ℃; ^{1}H NMR (400 MHz, $CDCl_3$) δ: 8.13～8.07 (m, 1H), 7.87～7.79 (m, 2H), 7.47～7.30 (m, 8H), 6.25 (d, J=3.3 Hz, 1H), 5.18 (s, 1H), 4.26 (q, J=7.1 Hz, 2H), 3.85～3.64 (m, 1H), 1.26 (td, J=7.1, 1.9 Hz, 3H); ^{13}C NMR (101 MHz, $CDCl_3$) δ: 170.83, 147.74, 133.47, 130.41, 129.33, 128.91, 128.81, 128.44, 128.20, 125.73, 120.21, 72.71, 66.08, 62.71, 14.06; HRMS (ESI) calcd for $C_{19}H_{20}N_3O_3$ $[M+H]^+$ 337.1426, found 337.1423.

3-Phenoxy-2-(4-phenyl-1*H*-1,2,3-triazol-1-yl)propan-1-ol (**3t**): 233 mg, brown oil, 79% yield. ^{1}H NMR (400 MHz, $CDCl_3$) δ: 7.90～7.84 (m, 1H), 7.76～7.67 (m, 2H), 7.44～7.30 (m, 5H), 7.02 (t, J=7.4 Hz, 1H), 6.95 (d, J=7.9 Hz, 2H), 4.80～4.70 (m, 1H), 4.63～4.50 (m, 2H), 4.28 (s, 1H), 4.12～4.03 (m, 2H); ^{13}C NMR (101 MHz, $CDCl_3$) δ: 158.13, 147.50, 130.15, 129.65, 128.83, 128.20, 125.59, 121.55, 121.41, 114.55, 68.87, 53.30; HRMS (ESI) calcd for $C_{17}H_{18}N_3O_2$ $[M+H]^+$ 295.1321, found 295.1321.

3-(Benzyloxy)-2-(4-phenyl-1*H*-1,2,3-triazol-1-yl)-propan-1-ol (**3u**): 232 mg, viscose oil, 75% yield. ^{1}H NMR (400 MHz, $CDCl_3$) δ: 7.82 (s, 1H), 7.71 (d, J=7.6 Hz, 2H), 7.42～7.30 (m, 8H), 4.61～4.52 (m, 3H), 4.44～4.37 (m, 1H), 4.35～4.26 (m, 1H), 4.18 (t, J=4.5 Hz, 1H), 3.55 (ddd, J=22.0, 9.7, 5.2 Hz, 2H); ^{13}C NMR (101 MHz, $CDCl_3$) δ: 147.41, 137.42, 130.26, 128.78, 128.53, 128.11, 128.02, 127.91, 125.57, 121.27, 73.58, 70.98, 69.18, 53.14; HRMS (ESI) calcd for $C_{17}H_{18}N_3O_2$ $[M+H]^+$ 309.1477, found 309.1475.

Supporting Information General information, experiment section in detail, and ^{1}H NMR and ^{13}C NMR spectra. The Supporting Information is available free of charge via the Internet at http://sioc-journal.cn.

References

[1] (a) Agalave, S. G.; Maujan, S. R.; Pore, V. S. *Chem. Asian. J.* **2011**, *6*, 2696.
(b) Bozorov, K.; Zhao, J.; Aisa, H. A. *Bioorg. Med. Chem.* **2019**, *27*, 3511.
(c) Buabeng, E. R.; Henary, M. *Bioorg. Med. Chem.* **2021**, *39*, 116140.

[2] (a) Saehlim, N.; Kasemsuk, T.; Sirion, U.; Saeeng, R. *J. Org. Chem.* **2018**, *83*, 13233.
(b) Zhang, W.; Xu, W.; Zhang, F.; Ma, C.; Ma, K.; Li, Y. *Chin. J. Org. Chem.* **2020**, *40*, 2338 (in Chinese).
(张文生, 许文静, 张斐, 马春玉, 马科友, 李焱, 有机化学, **2020**, *40*, 2338.)
(c) Liu, Q.; Lu, Y.; Bao, P.; Yue, H.; Wei, W. *Chin. J. Org. Chem.* **2020**, *40*, 4015 (in Chinese).
(刘启顺, 吕玉芬, 鲍鹏丽, 岳会兰, 魏伟, 有机化学, **2020**, *40*, 4015.)

[3] (a) Schock, M.; Braese, S. *Molecules* **2020**, *25*, 1009.
(b) Rodrigues, L. D.; Sunil, D.; Chaithra, D.; Bhagavath, P. *J. Mol. Liq.* **2020**, *297*, 111909.

[4] (a) Ra, A.; Fbz, B.; Mk, A.; Eb, C.; Ft, A. *J. Mol. Struct.* **2021**, *1232*, 130042.
(b) Yamada, M.; Takahashi, T.; Hasegawa, M.; Matsumura, M.; Ono, K.; Fujimoto, R.; Kitamura, Y.; Murata, Y.; Kakusawa, N.; Tanaka, M.; Obata, T.; Fujiwara, Y.; Yasuike, S. *Bioorg. Med. Chem. Lett.* **2018**, *28*, 152.

[5] Nejadshafiee, V.; Naeimi, H.; Zahraei, Z. *Chem. Data Collect.* **2020**, *28*, 100443.

[6] (a) Ge, C.; Sang, X.; Yao, W.; Zhang, L.; Wang, D. *Green Chem.* **2018**, *20*, 1805.
(b) Zhu, G.; Duan, Z.; Zhu, H.; Qi, M.; Wang, D. *Mol. Catal.* **2021**, *505*, 111516.
(c) Hu, W.; Zhang, Y.; Zhu, H.; Ye, D.; Wang, D. *Green Chem.* **2019**, *21*, 5345.
(d) Yao, W.; Zhang, Y.; Zhu, H.; Ge, C.; Wang, D. *Chin. Chem. Lett.* **2020**, *31*, 701.
(e) Hu, X.; Yang, B.; Yao, W.; Wang, D. *Chin. J. Org. Chem.* **2018**, *38*, 3296 (in Chinese).
(胡昕宇, 杨伯斌, 姚玮, 王大伟, 有机化学, **2018**, *38*, 3296.)

[7] (a) Camberlein, V.; Kraupner, N.; Bou Karroum, N.; Lipka, E.; Deprez-Poulain, R.; Deprez, B.; Bosc, D. *Tetrahedron Lett.* **2021**, *73*, 153131.
(b) Singh, M. S.; Chowdhury, S.; Koley, S. *Tetrahedron* **2016**, *72*, 5257.
(c) Guo, Y.; Liu, Y.; Wan, J. *Chin. Chem. Lett.* **2021**, Doi: 10.1016/j.cclet.2021.08.003.
(d) Ahmed, M.; Razaq, H.; Faisal, M.; Siyal, A.N.; Haider, A. *Synth. Commun.* **2017**, *47*, 1193.

[8] Totobenazara, J.; Burke, A. J. *Tetrahedron Lett.* **2015**, *56*, 2853.

[9] (a) Kalra, P.; Kaur, R.; Singh, G.; Singh, H.; Singh, G.; Pawan; Kaur, G.; Singh, J. *J. Organomet. Chem.* **2021**, *944*, 121846.
(b) Anbarasan, P.; Yadagiri, D.; Rajasekar, S. *Synthesis* **2014**, *46*, 3004.

[10] (a) Noshiranzadeh, N.; Emami, M.; Bikas, R.; Kozakiewicz, A. *New J. Chem.* **2017**, *41*, 2658.
(b) Kim, W.; Kang, M.; Lee, J.; Jeon, M.; Lee, S.; Lee, J.; Choi, B.; Cal, P. M. S. D.; Kang, S.; Kee, J.; Bernardes, G. J. L.; Rohde, J.; Choe, W.; Hong, S. *J. Am. Chem. Soc.* **2017**, *139*, 12121.
(c) Liu, Z.; Hao, W.; Gao, W.; Zhu, G.; Li, X.; Tong, L.; Tang, B. *Sci. China Chem.* **2019**, *62*, 1001.

[11] (a) Khalili, D.; Kavoosi, L.; Khalafi-Nezhad, A. *Synlett* **2019**, *30*, 2136.
(b) Talha, A.; Mourhly, A.; Tachallait, H.; Driowya, M.; El Hamidi, A.; Arshad, S.; Karrouchi, K.; Arsalane, S.; Bougrin, K. *Tetrahedron* **2021**, *90*, 132215.
(c) Alonso, F.; Moglie, Y.; Radivoy, G. *Acc. Chem. Res.* **2015**, *48*, 2516.
(d) Rani, G. S.; Vijay, M.; Prabhavathi Devi, B. L. A. *ChemistrySelect* **2019**, *4*, 10133.
(e) Bhaskaruni, S. V. H. S.; Maddila, S.; Gangu, K. K.; Jonnalagadda, S. B. *Arabian J. Chem.* **2020**, *13*, 1142.
(f) Rakhshanipour, M.; Eshghi, H.; Bakavoli, M. *Appl. Organomet. Chem.* **2020**, *34*, e5426.
(g) Tian, A; Luo, X.; Ren, Z.; Zhao, J.; Wang, L. *New J. Chem.* **2021**, *45*, 9614.

[12] Nasrollahzadeh, M.; Issaabadi, Z.; Tohidi, M. M.; Mohammad Sajadi, S. *Chem. Rec*. **2018**, *18*, 165.

[13] (a) Naeimi, H.; Shaabani, R. *Ultrason. Sonochem.* **2017**, *34*, 246.
(b) Gupta, A.; Jamatia, R.; Patil, R. A.; Ma, Y.-R.; Pal, A. K. *ACS Omega* **2018**, *3*, 7288.
(c) Mirza-Aghayan, M.; Saeedi, M.; Boukherroub, R. *Appl. Organomet. Chem.* **2020**, *34*, 5928.

[14] (a) Salam, N.; Sinha, A.; Roy, A. S.; Mondal, P.; Jana, N. R.; Islam, S. M. *RSC Adv*. **2014**, *4*, 10001.
(b) Xiong, X.; Chen, H.; Tang, Z.; Jiang, Y. *RSC Adv*. **2014**, *4*, 9830.
(c) Ghadamyari, Z.; Khojastehnezhad, A.; Seyedi, S. M.; Taghavi, F.; Shiri, A. *ChemistrySelect* **2020**, *5*, 10233.
(d) Deilam, R.; Moeinpour, F.; Mohseni-Shahri, F. S. *Monatsh. Chem.* **2020**, *151*, 1153.
(e) Kumar, A.; Verma, S.; Pathak, D. D. *J. Environ. Chem. Eng.* **2021**, *9*, 105791.

[15] (a) Huang, Q.; Zhou, L.; Jiang, X.; Zhou, Y.; Fan, H.; Lang, W. *ACS Appl. Mater. Interfaces* **2014**, *6*, 13502.
(b) Zhou, L.; Lang, W.; Jiang, X.; Huang, Q.; Yin, M. *Chin. J. Org. Chem*. **2015**, *35*, 2340 (in Chinese).

(周丽梅, 郎文成, 蒋晓慧, 黄强, 尹梦云, 有机化学, **2015**, *35*, 2340.)

[16] Saúl, N.; Elisa, L.; Edgar, M.; Luisa, F.; Loredo-Carrillo, Silvia, L. C. *Curr. Org. Chem.* **2020**, *24*, 536.

[17] (a) Sharma, N.; Choudhary, A.; Kaur, M.; Sharma, C.; Paul, S.; Gupta, M. *RSC Adv.* **2020**, *10*, 30048.
(b) Sultana, S.; Mech, S. D.; Hussain, F. L.; Pahari, P.; Borah, G.; Gogoi, P. K. *RSC Adv.* **2020**, *10*, 23108.
(c) Rout, L.; Kumar, A.; Dhaka, R. S.; Reddy, G. N.; Giri, S.; Dash, P. *Appl. Catal.*, *A* **2017**, *538*, 107.

[18] (a) Wang, Y.; Liu, J.; Xia, C. *Adv. Synth. Catal.*, **2011**, *353*, 1534.
(b) Sharghi, H.; Beyzavi, M. H.; Safavi, A.; Doroodmand, M. M.; Khalifeh, R. *Adv. Synth. Catal.* **2009**, *351*, 2391.
(c) Spiteri, C.; Moses, J. E. *Angew. Chem.*, *Int. Ed.* **2010**, *49*, 31.

(Cheng, F.)

